Green and Efficient Regeneration of Spent Lithium Batteries through Directional Leaching of Valuable Metals and Gradient Impurity Separation

Yuan Jin, Jinxia Yao, Sixuan Xiang, Guangli Li*

School of Biological Science and Medical Engineering, Hunan University of Technology, Zhuzhou, 412007, China.

* Corresponding authors.

e-mail: guangli010@hut.edu.cn (G. Li)

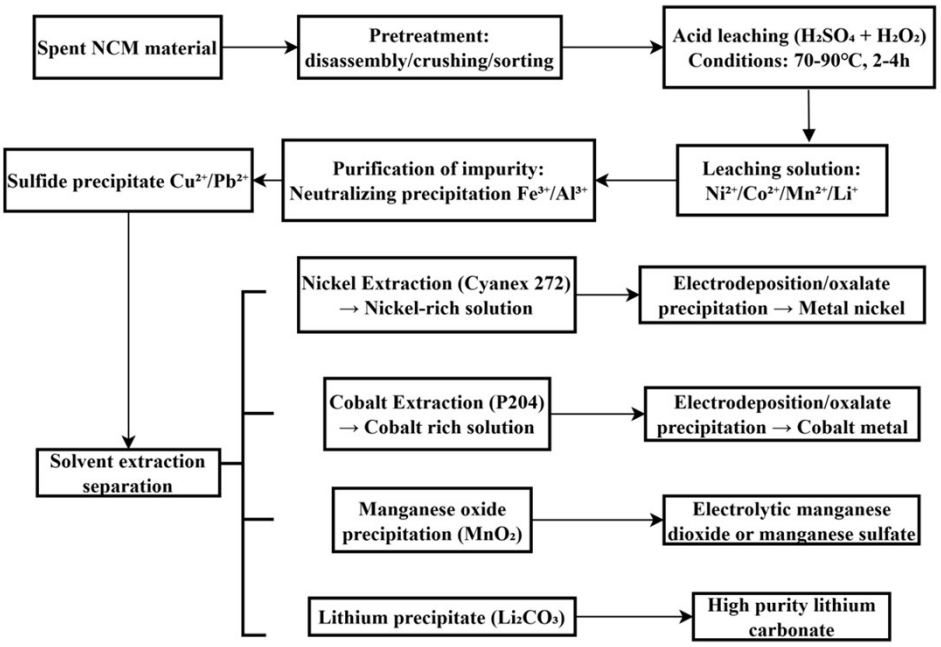

Fig. S1 The conventional hydrometallurgical process for the recovery of valuable metals from waste NCM materials.

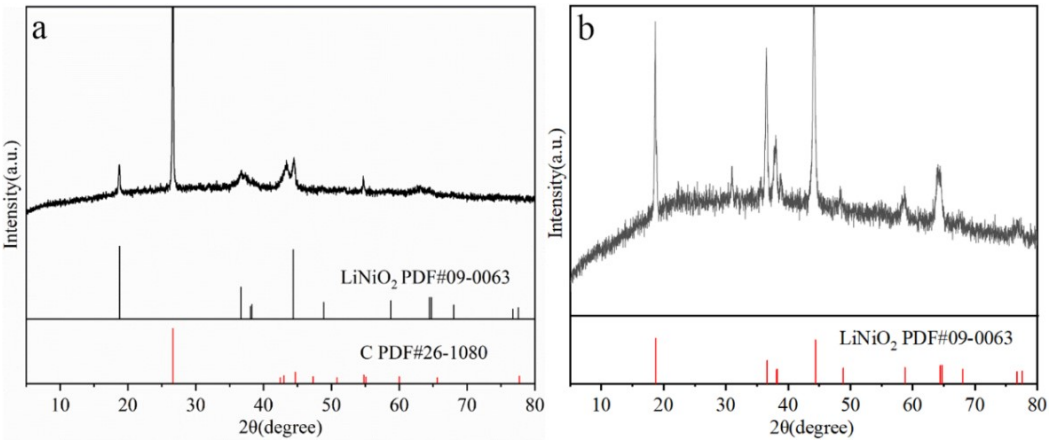

Fig. S2 (a) XRD pattern of the raw material powder from spent lithium-ion batteries; (b) XRD pattern of the battery powder following calcination at 800℃ under an oxygen atmosphere.

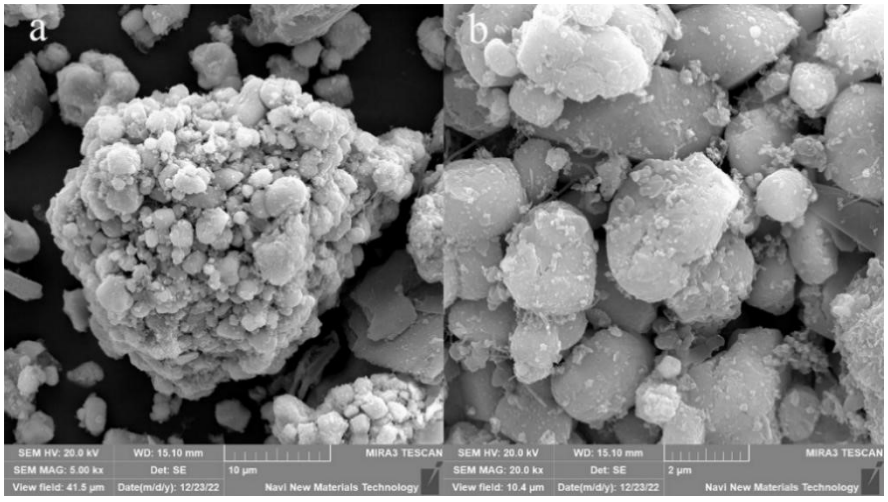

Fig. S3 SEM images of the raw material powder from spent lithium-ion batteries

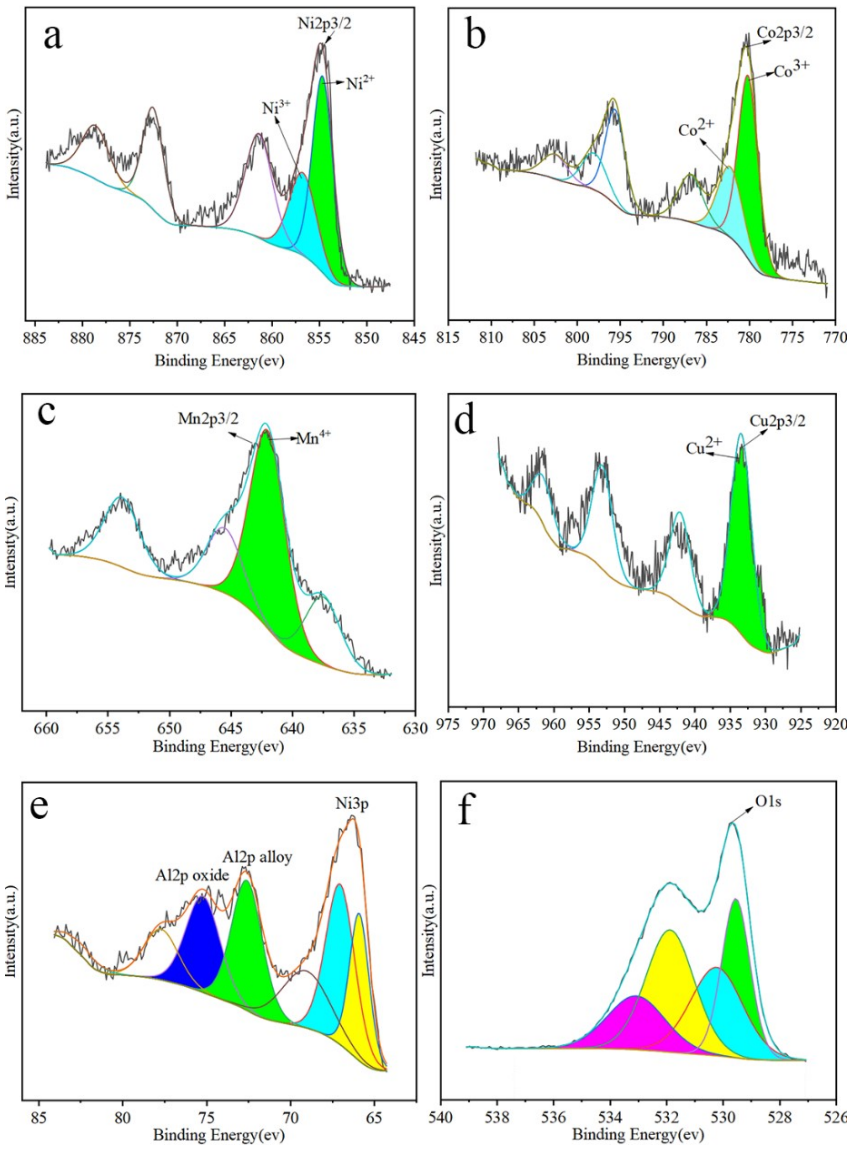

Fig. S4 XPS assessment of the raw material powder from spent lithium-ion batteries:

(a) Ni, (b) Co, (c) Mn, (d) Cu, (e) Al, (f) O.

The XRD pattern presented in **Fig. S2** indicates that the raw material exhibits a typical ternary layered structure of Li ($Ni_xCo_yMn_2$) O_2, along with characteristic peaks of graphite. Following oxidation calcination at 800℃, the original structure is disrupted, resulting in the formation of metal oxide phases such as NiO and Co_3O_4, which provide a reaction interface for subsequent reduction-leaching processes. The SEM image in **Fig. S3** demonstrates that the raw materials consist of irregular micron-

sized particles that exhibit agglomeration, thereby underscoring the necessity of mechanically activating and reducing their size to D_{90} < 50 μm, as discussed in the main text, to enhance reaction kinetics. The XPS analysis in **Fig. S4** elucidates the initial chemical states of each element, identifying Ni^{2+}/Ni^{3+}, Co^{3+}, and Mn^{4+} as the predominant valence states, while Cu and Al are found in mixed oxidation/metal and trivalent states, respectively. This information provides a crucial basis for processes such as carbon-thermal reduction, selective phase transformation, alkaline aluminum removal, and copper gradient extraction, as detailed in the article.

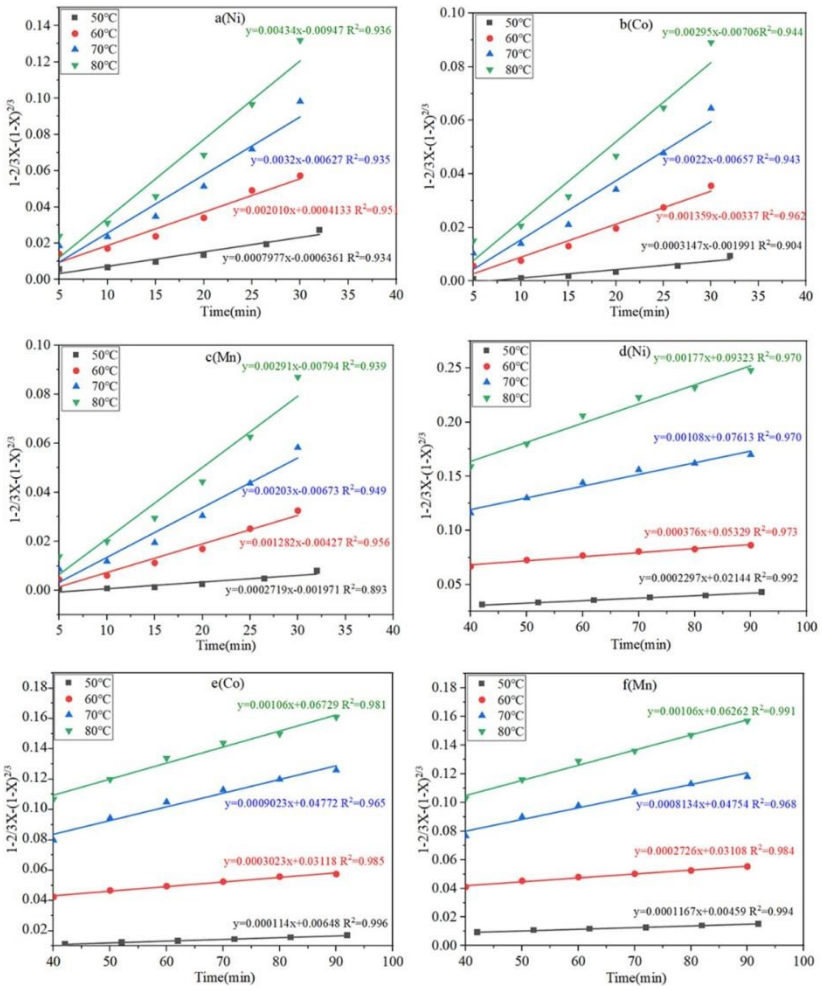

Fig. S5 Illustrates the correlation between the diffusion control models and time t for Ni, Co, and

Mn at different temperatures and time periods: (a) Ni, 0-40 min, (b) Co, 0-40 min, (c) Mn, 0-40 min, (d) Ni, 40-90 min, (e) Co, 40-90 min, (f) Mn, 40-90 min.

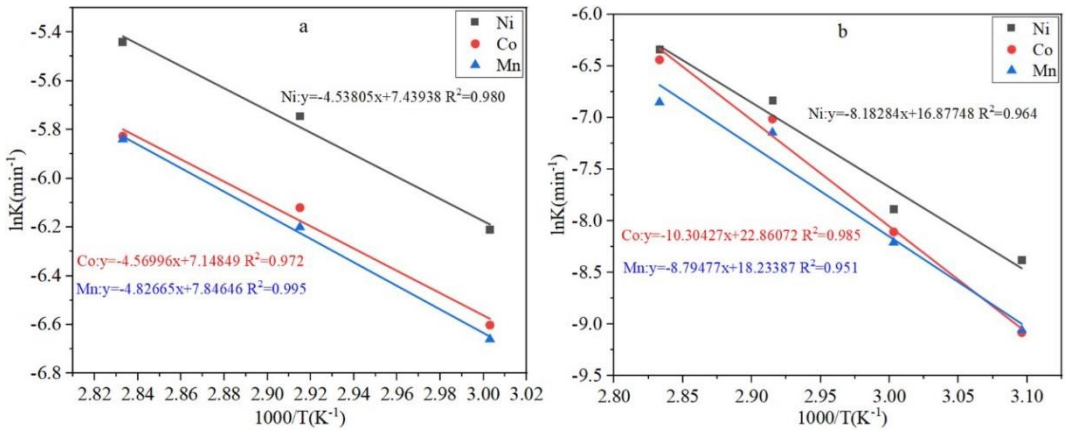

Fig. S6 The relationship between lnk and 1/T derived from the diffusion control models for Ni, Co, and Mn over two time intervals: (a) 0-40 minutes and (b) 40-90 minutes.

Table1 Summary of operational conditions for the metal recovery from Li-ion batteries

Sample	Experimental method	Letching reagents	Concentration of Li	Efficiency (%)	Ref.
spent lithium-ion batteries	Hydrothermal reduction-ammonia leaching	$(NH_4)_2SO_3$ NH_3-NH_4Cl	90.3%	Co:100% Ni:98.3% Al、Mn not leached	Ref. 1
$Li(Ni,Co,Mn)_{1/3}O_2$	High temperature leaching-ammonia circulation system	NH_3-$(NH_4)_2SO_4$-Na_2SO_3	95.3%	Ni:89.8% Co:80.7%Mn:4.3 %	Ref.2
spent lithium-ion batteries	Ternary leaching system	NH_3-$(NH_4)_2SO_3$ -NH_4HCO_3	60.53%	Ni：96.3% Co：80.9%	Ref. 3
spent lithium-ion batteries	**CO_2-assisted green leaching- step separation of impurities**	**H_2SO_4-H_2O_2 M5640 P204**		**Ni:98.54%Co:97. 37%Mn:98.0%**	**This work**

Ref.1: Wang, Shubin, et al. Reduction-ammoniacal leaching to recycle lithium, cobalt, and nickel from spent lithium-ion batteries with a hydrothermal method: Effect of reductants and ammonium salts. *Waste Management* 102 (2020): 122-130.

Ref.2: Zheng, Xiaohong, et al. Spent lithium-ion battery recycling–Reductive ammonia leaching of metals from cathode scrap by sodium sulphite. *Waste management* 60 (2017): 680-688.

Ref.3: Wu, Caibin, et al. Recycling valuable metals from spent lithium-ion batteries by

ammonium sulfite-reduction ammonia leaching. *Waste Management* 93 (2019): 153-161.

Compared with the recent research on carbon-thermal reactions.

Comparison dimension	This Work	Ref. 4	Ref. 5
Core method	Carbon thermal reduction (at 900 °C) + CO_2-assisted water immersion	Carbon thermal reduction (at 950 °C) + Atmospheric water immersion	CO_2 -mediated carbothermal reduction (800 °C) + CO_2 saturated leaching
Li recovery rate	88.5%	95.7% (handled by NMC alone)	99.8%
Reaction temperature	900 °C	950 °C	800 °C
Recycling of TM	There are subsequent processes that can efficiently recover Ni (98.54%), Co (97.37%), and Mn (98.00%).	There is no subsequent recovery. The research focus is on selective lithium extraction, and TM remains in the slag.	Not covered. The research focus is on selective lithium extraction and the preparation of high-purity Li_2CO_3.
Removal of impurities	Gradient separation was achieved through M5640 and P204, with a total impurity removal rate of over 99%.	Not involved	Not involved
Degree of Process Integration	Highly integrated, with a complete closed-loop process covering lithium extraction, TM recovery and impurity removal.	Partial integration, focusing only on the lithium extraction step.	Partial integration, focusing only on the lithium extraction step under CO_2 regulation.

Ref.4: Perdana, I., et al. "Lithium recovery from mixed spent LFP-NMC batteries through atmospheric water leaching." Scientific Reports, 2025, 15, 2591.

Ref.5: Hu, G., et al. "CO_2-mediated carbothermal reduction coupled with CO_2-saturated leaching for selective lithium recovery from spent lithium-ion batteries." Separation and Purification Technology, 2025, 358, 131200.

Reagent consumption calculation (based on 1 kg of black powder)

Reagent	This Work	Typical hydrometallurgical process	Degree of reduction
H_2SO_4	0.39 kg	0.70 kg	↓44%
NaOH	0.29 kg	0.63 kg	↓54%
H_2O_2	0.12 kg	0.20 kg	↓40%

The calculation includes all the main reagents and auxiliary reagents (extractants, diluents, etc.) throughout the entire process. The results support the conclusion that "acid and base consumption is reduced by approximately 40%".

Table 2 Composition and content of powder materials from spent lithium-ion batteries. (mass fraction, %)

Ni	Co	Mn	Cu	Ba	Fe	Ca	Zn
18.65	8.104	10.216	5.67	0.467	0.3043	0.133	0.007

Table 3 Extraction rate of lithium after calcination at different temperature under N_2 conditions.

Temperature	500℃	600℃	700℃	800℃	900℃	1000℃
Extraction rate (%)	47.23	61.20	64.96	77.88	88.53	90.53

Table 4 Element composition and content in the powder of spent lithium-ion batteries after carbon thermal reduction, lithium extraction, alkaline leaching, and oxygen calcination.

Element	Ni	Co	Mn	Li	Cu	Al	Zn	Ca	Fe
Content (wt%)	34.02	16.49	18.79	0.97	10.19	0.348	0.259	0.17	0.50

Table 5 Element (al) composition and concentration in the leaching solution of spent lithium-ion battery powder after leaching.

Element	Ni	Co	Mn	Li	Cu	Al	Zn	Ca	Fe
Concentration (g/L)	77.78	37.25	42.72	2.22	23.64	0.807	0.495	0.362	1.00

Table 6 Element (al) composition and concentration in the solution after copper

extraction with M5640.

Element	Ni	Co	Mn	Li	Cu	Al	Zn	Ca	Fe
Concentration (g/L)	77.06	36.97	42.24	2.22	0.02	0.81	0.49	0.36	0.95